

Cytotoxicity and genotoxicity of coated-gold nanoparticles on freshwater algae *Pseudokirchneriella subcapitata*

Ntombikayise Mahaye, Samuel K. Leareng, Ndeke Musee¹

Emerging Contaminants Ecological and Risk Assessment (ECERA) Research Group, Department of Chemical Engineering, University of Pretoria, Private Bag X20, Hatfield 0028, Pretoria, South Africa

Highlights

- nAu can inhibit or promote growth and chlorophyll *a* content of *P. subcapitata*.
- No significant cellular effects were observed except at 1 mg/L for 5 nm BPEI.
- nAu induced genotoxic effects to algae although none apparent at cellular level.
- Under chronic exposure a reverse on nAu-induced genotoxic effects may occur.

•

nAu is a potential genotoxic nano-pollutant for algae.

Abstract

Gold engineered nanoparticles (nAu) are increasingly detected in ecosystems, and this raises the need to establish their potential effects on aquatic organisms. Herein, cytotoxic and genotoxic effects of branched polyethylenimine (BPEI)- and citrate (cit)-coated nAu (5, 20, and 40 nm) on algae *Pseudokirchneriella subcapitata* were evaluated. The apical biological endpoints: growth inhibition and chlorophyll *a* (Chl *a*) content were investigated at 62.5–1000 µg/L over 168 h. In addition, the apurinic/aprimidinic (AP) sites, randomly amplified polymorphic deoxyribonucleic acid (RAPD) profiles, and genomic template stability (GTS) were assessed to determine the genotoxic effects of nAu. The results show algal growth inhibition at 5 nm BPEI-nAu up to 96 h, and thereafter cell recovery except at the highest concentration of 1000 µg/L. Insignificant growth reduction for cit-nAu (all sizes), as well as 20 and 40 nm BPEI-nAu, was observed over 96 h, but

¹ Corresponding author: email: ndeke.musee@up.ac.za or museen2012@gmail.com

growth promotion was apparent at all exposures thereafter except for 40 nm BPEI-nAu at 250 µg/L. A decrease in Chl *a* content following exposure to 5 nm BPEI-nAu at 1000 µg/L corresponded to significant algal growth reduction. In genotoxicity studies, a significant increase in AP sites content was observed relative to the control – an indication of nAu ability to induce genotoxic effects irrespective of their size and coating type. For 5 nm- and 20 nm-sized nAu for both coating types and exposure concentrations no differences in AP sites content were observed after 72 and 168 h. However, a significant reduction in AP sites was observed following algae exposure to 40 nm-sized nAu (irrespective of coating type and exposure concentration) at 168 h compared to 72 h. Thus, AP sites results at 40 nm-size suggest likely DNA damage recovery over a longer exposure period. The findings on AP sites content showed a good correlation with an increase in genome template stability and growth promotion observed after 168 h. In addition, RAPD profiles demonstrated that nAu can induce DNA damage and/or DNA mutation to *P. subcapitata* as evidenced by the appearance and/or disappearance of normal bands compared to the controls. Therefore, genotoxicity results revealed significant toxicity of nAu to algae at the molecular level although no apparent effects were detectable at the morphological level. Overall, findings herein indicate that long-term exposure of *P. subcapitata* to low concentrations of nAu may cause undesirable sub-lethal ecological effects.

Keywords: Genomic template stability, RAPD, apurinic/apyrimidinic sites, *Pseudokirchneriella subcapitata*, gold engineered nanoparticles

1. Introduction

Increasing use and applications of engineered nanoparticles (ENPs) in commercial products (e.g., cosmetics, paints, medical devices, packaging, catalysts, etc), and their subsequent emission into the environment necessitates an understanding of their potential effects on aquatic biota (Klaine et al. 2008; Scown et al. 2010; Châtel and Mouneyrac 2017). Among priority ENPs for immediate toxicity testing are gold ENPs (nAu) (OECD, 2010) as they are widely used in consumer products and industrial applications (Piccinno et al. 2012; Hansen et al. 2016). For example, to date there are numerous applications of nAu in various fields such as biomedical imaging and detection (Copland et al., 2004; Jiang et al., 2006), cancer diagnostics and therapy (El-Sayed et al., 2005), catalysis (Thompson 2007). This is attributed to their relatively simple surface functionalization

(Bodelón et al., 2017). However, nAu are among the least studied for their potential negative environmental effects (Chen et al., 2015), especially genetic effects on aquatic biota (Mahaye et al., 2017). Only a handful of studies have linked the physicochemical properties of ENPs (e.g., size, surface coating) to the observed genotoxicity in aquatic organisms (Mahaye et al., 2017). nAu have a wide range of sizes and coatings, which could affect their interactions with the environment or with biological structures and, thus, modify their toxic effects (Vales et al., 2020). For various biological applications e.g., cancer therapy, nAu are generally coated with different polymers e.g., branched polyethylenimine (BPEI), citrate (cit), etc., to reduce aggregation and/or dissolution and to maintain ENPs' desired properties (Anantha et al., 2011). However, the chemistry of ENPs' coatings can influence the chemical and biological activities of ENPs once they are released into the aquatic environment (Perreault et al., 2012; Qiu et al., 2015; Kim et al. 2016; Mahaye, 2019, Sen et al., 2020). For example, Perreault et al., (2012) observed that polymer-coated nCuO were more toxic to the algae *Chlamydomonas reinhardtii* compared to uncoated nCuO due to increased membrane permeability. Qiu et al., (2015) observed coating-dependent gene expression patterns from negatively charged mercaptopropionic acid (MPA) and polyallylamine hydrochloride (PAH)-coated nAg to *Shewanella oneidensis* and *Daphnia magna*.

To date, studies on the toxicological outcomes of ENPs on aquatic organisms including fish (Qiang et al., 2020), crustaceans (Danabas et al., 2020), higher aquatic plants (Thwala et al., 2016), and algae (Sendra et al. 2017; Ghazaei and Shariati 2020) have focused broadly on morphological- and physiological-level effects (Kahru and Dubourguier 2010; Chen et al., 2015; Mahaye et al., 2017). For example, algal morphological endpoints such as growth rate (Gao et al. 2016; Chen et al. 2018), biomass (Angel et al. 2015; Aruoja et al. 2015; Sendra et al. 2017; Kleiven et al. 2019), and chlorophyll content (Chen et al. 2012; Ghazaei and Shariati 2020) are well documented. However, in the absence of genetic endpoints e.g., DNA damage, chromosomal aberrations, chromosome damage, and loss, among others (Mahaye et al. 2017) they offer limited insights on the effects of pollutants to target organisms (Oberholster et al. 2016).

Molecular studies are essential for assessment of ENPs impact on aquatic biota, especially at very low environmentally relevant concentrations (ng/l to ug/l) in as shown in both modeling (Musee, 2011, Caballero-Guzman and Nowack 2018), and experimental (Peters et al. 2018; Zhao et al., 2020) studies. For example, nAu concentrations detected in the environment by Bäuerlein et al.,

(2017) ranged from 0.13 to 0.25 µg/L. At these concentrations, effects to aquatic organisms may not be apparent at the morphological level, but may induce sub-lethal effects, including DNA damage with far-reaching ecological implications. For example, de Alteriis et al. (2018) reported DNA damage following exposure of *Saccharomyces cerevisiae* to 50 µg/L nAu, but no growth inhibition was apparent. DNA damage was observed without lactate dehydrogenase (LDH) leakage following exposure of zebrafish to titanium dioxide ENPs (nTiO₂) (Bayat et al. 2015). In addition, 1, 10, and 100 mg/L nTiO₂ exposure induced DNA strand breaks in *Piaractus mesopotamicus* with neither mortality nor abnormal behavioural symptoms being observed (Clemente et al., 2013). These studies suggest ENPs can exert damage to current populations at sub-lethal levels, with likely transfer of mutagenic effects to subsequent generations (Bolognesi and Hayashi 2011; Deavaux et al. 2011). This, in turn, can alter ecological functions (Bolognesi and Cirillo 2014) e.g., organisms' development, growth, and reproduction (Ginebreda et al., 2014) with consequent lack of food sources for higher organisms, and imbalances within a given ecosystem.

To fully understand the mode of ENPs' toxicity, genotoxicity data can offer valuable insights when used together with higher level cellular biological response data (e.g. growth) (Demir et al. 2014; Amaeze et al. 2015; Golbamaki et al. 2015; Koehlé-Divo et al. 2018). It is with this understanding that the Organisation for Economic Co-operation and Development (OECD) recommended genotoxicity assessment of ENPs for regulatory and risk assessment purposes (Nanogenotox, 2013; ANSES, 2014); however, to date, only limited data have been reported for aquatic biota (Mahaye et al., 2017) unlike in mammalian systems (Magdolenova et al. 2014; Golbamaki et al. 2015; Samadian et al. 2020).

Random amplified polymorphic deoxyribonucleic acid by PCR (RAPD- PCR) analysis is one of the reliable genotoxicity methods that can screen for changes in DNA profiles, and evaluate genomic instability. Key advantages of RAPD-PCR include exclusion of prior knowledge for the genome, use of short primers (10 bp sequence) unlike Real Time-PCR, the ease and efficiency in detecting subtle changes in genomic DNA (Manna et al 2017). Several studies have applied RAPD-PCR to determine the genotoxicity of ENPs to aquatic biota e.g., bacteria (Amjady et al. 2016; Załęska-Radziwiłł and Duskocz 2016), mussel (Rocco et al. 2015b), and fish (Geffroy et al. 2012; Rocco et al. 2015a). Due to the link between the formation of abasic (apurinic/aprimidinic) AP

sites and DNA damage, evaluation of AP sites content may provide a measure of mutagen-induced DNA damage (Boturny et al., 1999). In brief, AP sites arise in DNA at a significant rate by spontaneous base loss (depurination) due to oxidative DNA damage (Demple and Harrison, 1994, Feng et al. 2019). The presence and size of AP sites signal the extent of DNA damage, which if unrepaired, may eventually lead to cell death (Loeb and Preston 1986; Seiple et al. 2008, Feng et al. 2019). This assay has been used to investigate the role of trehalose in persister formation in *E. coli* (Kuczyńska-Wiśnik et al., 2015). Findings showed that the lack of trehalose in the DotsA mutant resulted in oxidative stress, manifested by increased membrane lipid peroxidation after heat shock. The AP sites assay merits in genotoxicity are well established (Kuczyńska-Wiśnik et al., 2015; Jang et al., 2017; Wang et al., 2018), however, to the authors' knowledge it has not been applied for ENPs' environmental effects assessment.

Despite limited data on genetic biomarkers of ENPs, for example, to algae; evidence demonstrates they can aid to identify potential risks of bulk chemical pollutants in aquatic systems with resultant desirable outcomes including the protection of the human health (Oberholster et al. 2016). Therefore, we hypothesize that nAu may induce genotoxicity in algae even in cases where no biological effects are apparent at the morphological level. The aim of the study is to assess nAu induced genotoxicity on the freshwater green algae *Pseudokirchneriella subcapitata* using RAPD-PCR and AP sites analysis. The specific study objectives entailed assessing the influence of: (i) low and close to environmental relevant but detectable nAu concentrations (62.5–1000 µg/L), (ii) physicochemical properties of nAu (e.g. size, and surface coating), and (iii) assessment of the linkage between cellular and molecular level toxicological outcomes. Algae were chosen as exposure organism because they play a significant role as primary producers and forms the basis of all food chains (Sadiq et al. 2011), has short generation time and is highly sensitive to pollutants; hence, serves as an excellent aquatic model organism for ecotoxicity assessments (Ji et al. 2011; Chen et al. 2012).

2. Materials and Methods

2.1 Characterization of nAu

Commercial citrate (cit)- and branched polyethylenimine (BPEI)-coated nAu each sized 5, 20, and 40 nm were purchased from Nanocomposix (San Diego, United States). Size and morphology were

previously characterized and reported elsewhere (Mahaye, 2019). Aggregation kinetics of nAu in 10% BG-11 algal media (Slabbert, 2004) was determined by measuring the hydrodynamic diameter (HDD) and zeta (ζ) potential using dynamic light scattering (DLS; Malvern Zetasizer Nano ZS, Malvern Instruments, UK) over 72 h.

2.2 Pseudokirchneriella subcapitata

The Algaltoxkit FTM kit (MicroBioTests Inc., Gent, Belgium) was purchased from ToxSolutions (Johannesburg, South Africa). De-immobilization of *P. subcapitata* from the beads in the kit was performed according to the manufacturer's instructions (detailed method provided in SI-1). Further, chemicals used to prepare 10% BG-11 algal media, reference tests aimed to ascertain the sensitivity of algae growth as well as the algal growth and chlorophyll *a* (Chl *a*) content effects of ENPs are described in sections SI-2 to SI-4, respectively.

2.3 Genotoxicity of nAu to P. subcapitata

To carry out genotoxicity studies, exponentially growing *P. subcapitata* were exposed to three nAu concentrations (62.5, 250, and 1000 $\mu\text{g/L}$) over 168 h as described in SI-1. Herein, *P. subcapitata* exposures to nAu were done following the standard algal test of 72 h (Slabbert, 2004; OECD 201), or 96 h (US EPA, 1978, 1989). Moreover, the exposure time was increased to 168 h. This was to gain insights on whether likely damage at the molecular level is permanent or recovery may occur over an extended period. Standard US EPA flask test method (US EPA, 1978, 1989) was found to generate inadequate biomass for genotoxicity analysis as it requires 10 000 cells/mL as initial inoculum. To generate sufficient biomass for genotoxicity analysis, the Direct Estimation of Ecological Effects Potential (DEEEP) toxicity testing protocol was used (Slabbert, 2004) as it requires an inoculum of 200 000 cells/mL which gives an adequate biomass for DNA damage analysis. For negative controls, exposures for algae were without nAu. All experiments were done in triplicates.

2.3.1 DNA isolation and visualization

After exposing *P. subcapitata* to nAu over 72 and 168 h, algal DNA was extracted using the MasterPureTM DNA purification kit (Epicentre, USA) following the manufacturer's instructions. Importantly, three minor modifications were made. These entailed, first, sample incubation was

increased from 15 min to 30 min at 65 °C to improve cell lysis. Secondly, 1 µL was increased to 3 µL RNase cocktail to increase the efficiency of cell lysis, and finally, an additional 1 h incubation step at -20 °C was done after the addition of isopropanol to improve DNA precipitation. DNA precipitation and purification were done in accordance with the prescribed manufacturer's protocol. DNA purity (OD_{260}/OD_{280}) and concentration (ng/µL) were determined using a Nanodrop 2000 Spectrophotometer (Thermo Scientific, US). The ratio of $OD_{260}/OD_{280} \geq 1.7$ denotes contaminant-free DNA, and < 1.7 signifies the presence of contaminants (Barbas et al., 2007). Three-µL of the extracted DNA was separated using 1.5% ethidium bromide-stained agarose gel dissolved in 1 X TAE buffer (Tris-acetate-EDTA buffer, pH 7.5) at 90 mV for 45 min. And thereafter, DNA visualization was done using a UV transilluminator (Bio-Rad, USA).

2.3.2 DNA amplification

In this study, four 10-base pairs RAPD primers, namely; OPA9 (5'-GGGTAACGCC -3'), OPB10 (5'-CTGCTGGGGAC-3'), OPB1 (5'-GTTTCGCTCC-3'), and OPB14 (5'-TCCGCTCTGG-3') were initially tested for RAPD-PCR. This is because these primers have been previously applied in genotoxicity studies, including algal studies (Atienzar et al., 2002; Nyati et al., 2013). However, herein only two primers showed stable results as well as greater reproducibility and were selected for this study, viz.: OPB1 and OPB14. Primers were purchased from Inqaba Biotechnical Industries (Pty) Ltd (South Africa). The first experimental phase entailed preliminary studies aimed to optimise reagent(s) volumes, and more details are provided in SI-5. For example, the primer and DNA volumes were increased to enhance the DNA-primer binding and to obtain clearer bands (SI-5).

Amplification was performed in 25 µL reaction volumes consisting of 1 µL primers, 6 µL deionized water (DIW), 2.5 µL bovine serum albumin (BSA), 12.5 µL ready mix, and 3 µL genomic DNA using a PCR thermocycler (T100™ Thermal Cycler, Bio-Rad, Singapore). For the negative control, no genomic DNA was added. Further, amplification using the RAPD primers was carried out under the following conditions: warming step at 94 °C for 5 min, 40 cycles of denaturation at 94 °C for 45 s, annealing (46.8 °C for OPB1 and 44.3 °C for OPB14) for 30 s, extension 68 °C for 1 min, and a final extension at 68°C for 10 min. The amplified products were kept at 4 °C until gel electrophoresis analysis was performed. Bands were separated on a 1.5%

ethidium bromide-stained agarose gel at 80 mV for 2 h and then visualised using a UV transilluminator (Bio-Rad, USA). A 10-kb universal DNA Ladder (Kapa Biosystems, South Africa) was used as the molecular weight standard. RAPD data analysis was performed by comparing the PCR product profiles for treated and control samples. The GTS% was calculated using the expression (Atienzar et al. 2002):

$$\text{GTS\%} = \left(1 - \frac{a}{n}\right) * 100 \quad (1)$$

where a is the average number of RAPD polymorphic bands detected in ENPs-treated samples, and n is the total bands in the controls. Polymorphisms in RAPD profiles include deletion of a normal band and induction of a new band in comparison to the control RAPD profiles. GTS% of ENPs-treated samples was calculated, and changes of genomic stability were expressed as a percentage of controls set to 100%.

2.3.3 Detection of AP sites content

DNA lesions were investigated using the DNA Damage–AP site–Assay Kit (ab211154: Colorimetric, Biocom Africa) in accordance with the manufacturer’s instructions. The assay uses an Aldehyde Reactive Probe (ARP) designed to specifically react with an aldehyde group on the open-ring form of AP sites. This was followed by colorimetric detection with a sensitivity range of 4-40 AP sites per 1×10^5 base pairs (bp). AP sites content was determined by comparing the absorbance (at OD₄₅₀) between treated and untreated samples with a standard curve generated by the DNA standards containing predetermined AP sites.

2.4 Data Analysis

All data herein are presented as mean \pm standard deviation (SD). Differences between exposure treatments were tested by analysis of variance (ANOVA) using GraphPad Prism V7.04 (GraphPad Prism Software Inc., La Jolla, USA). Differences between samples were considered statistically significant when $p < 0.05$. The 72-h EC₅₀ values were calculated using Algaltookit Data Treatment spreadsheet (MicroBioTest inc., Belgium).

3. Results and Discussion

3.1 Nanoparticles characterization

Cit- and BPEI-nAu had mixed morphologies with spheres being more predominant compared to rods and pentagon shapes (Figure S1a-f) (Mahaye, 2019). The HDD results indicated the aggregation of nAu in 10% BG-11 media over 72 h (Figure 1a, c). Both 5 and 20 nm-sized cit- and BPEI-coated nAu showed significant increases of HDD over 72 h compared to 40 nm-sized ones. However, cit-coated nAu had higher aggregate sizes compared to BPEI-coated ones irrespective of exposure duration (Figures 1a, c). Conversely, 40 nm BPEI-nAu had no significant changes in HDD over the exposure period compared to cit-coated nAu (Figure 1c). This suggests that the 40 nm BPEI-nAu were stable in 10% BG-11 media, and these results are similar to previous findings (Iswarya et al. 2016; Chen et al. 2019).

Irrespective of coating type, all nAu had negative ζ -potential in 10% BG-11 media (Figure 1b, d). No marked differences in ζ -potentials were observed and within a narrow range of -5 to -14 mV. These ζ -potentials were considered too low relative to ± 30 mV known to stabilize ENPs suspensions (O'Brien and White, 1978; Hitchman et al., 2013; Lowry et al., 2016). Hence, the low ζ -potentials may account for nAu instability in 10% BG-11 media. The ζ -potential and HDD results indicated that coating had an influence on nAu stability as cit-nAu were less stable compared to BPEI-nAu. The BPEI-coated nAu were more stable likely due to high steric hindrances, and a large number of functional groups e.g., amino groups compared to the cit-coated ones (Cao et al., 2015; Liu et al., 2016). Similarly, in earlier works, BPEI coating was observed to induce higher stability of nAu under a physiological isotonic medium (phosphate-buffered saline) (Cho et al., 2019).

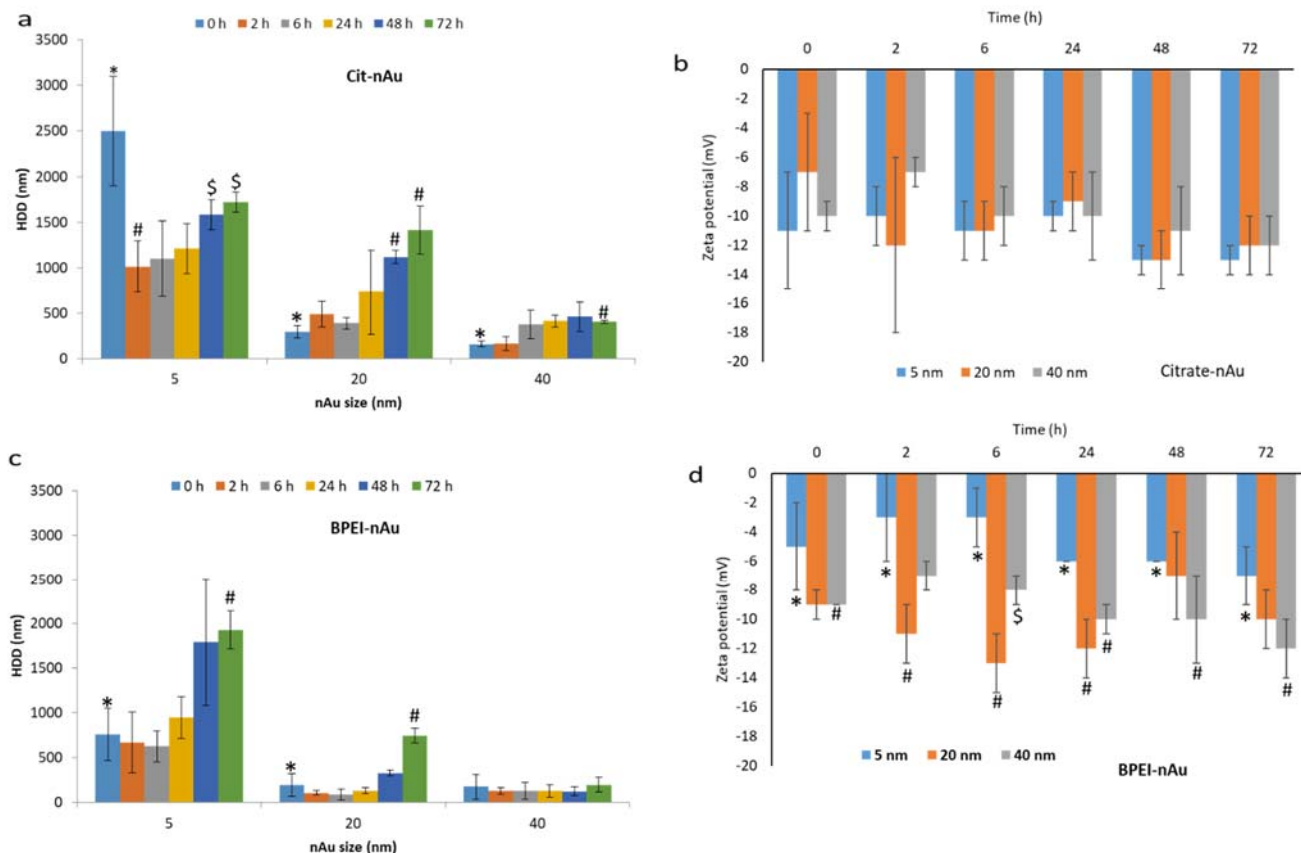


Figure 1: HDD (a, c), and ζ potentials (b, d) for nAu at 1000 $\mu\text{g/L}$ in 10% BG-11 algal media measured using DLS over 72 h. Data are presented as mean ($n = 3$), bars denote standard deviations (SD), and different symbols denote significant differences ($p < 0.05$) between nAu sizes per time period. nAu concentrations $< 1000 \mu\text{g/L}$ were below detection limit using Zetasizer.

3.2 Effect of nAu on *P. subcapitata* growth

Results of differently coated- and sized-nAu demonstrated induction of algal growth inhibition following exposure for up to 96 h, and growth promotion (hormesis effect) post 96 h (Figure 2). Growth inhibition was observed for 5 nm-sized nAu (irrespective of coating type) post 24 h up to about 96 h (Figures 2 a, b); but induced growth promotion after 96 h. However, at the highest exposure concentration of 1 000 $\mu\text{g/L}$, a decrease in cell density compared to the control was apparent over 168 h for 5 nm cit- ($p > 0.05$), and 5 nm BPEI-nAu ($p < 0.05$). At higher nAu sizes of 20 and 40 nm (irrespective of coating type), insignificant growth reduction was observed for 96 h exposures (Figures 2 c –f). In addition, insignificant growth promotion ($p > 0.05$) was observed

irrespective of exposure concentration after 96 h (Figures 2 c –f); except for 40 nm-sized BPEI-nAu at 250 $\mu\text{g/L}$ (Figure 2f)-where growth inhibition ($p > 0.05$) was apparent over 168 h. Overall, findings herein indicate that the effects of nAu on algae were size- and coating type-dependent.

The EC_{50} for 5 nm BPEI-nAu to *P. subcapitata* was 980 $\mu\text{g/L}$, but could not be calculated for other nAu types as growth inhibition did not reach 50% in addition to growth promotion induced post 96 h. These findings are similar to those reported by Dědková et al., (2014) where growth promotion was observed on *P. subcapitata* exposed to polyvinylpyrrolidone (PVP) coated-nAu (43.67 nm) at 5 – 80 $\mu\text{g/}$ for 72 h. Surface coating exerts a significant influence on ENPs interactions with algae (Kalman et al. 2015; Zhang et al. 2020), and therefore, the resultant toxicities are coating type- and form-dependent (Musee et al., 2020). For example, exposure of *Chlorella vulgaris* to PVP- and cit-coated nAg exhibited similar toxicity (IC_{50} : 9.3 and 9.2 mg/L, respectively) compared to polyethylene glycol (PEG)-nAg (IC_{50} : 49.3 mg/L) (Kalman et al. 2015). Further, exposure of *C. vulgaris* to 20 nm BPEI- and cit-coated nAg revealed the uptake rate constants of BPEI-nAg were ~ 20 times higher relative to cit-nAg, and BPEI-nAg were more effectively bioaccumulated than cit-nAg (Zhang et al. 2020). These findings together with our current results indicate the significant role of surface coating play on the effects of ENPs on algae.

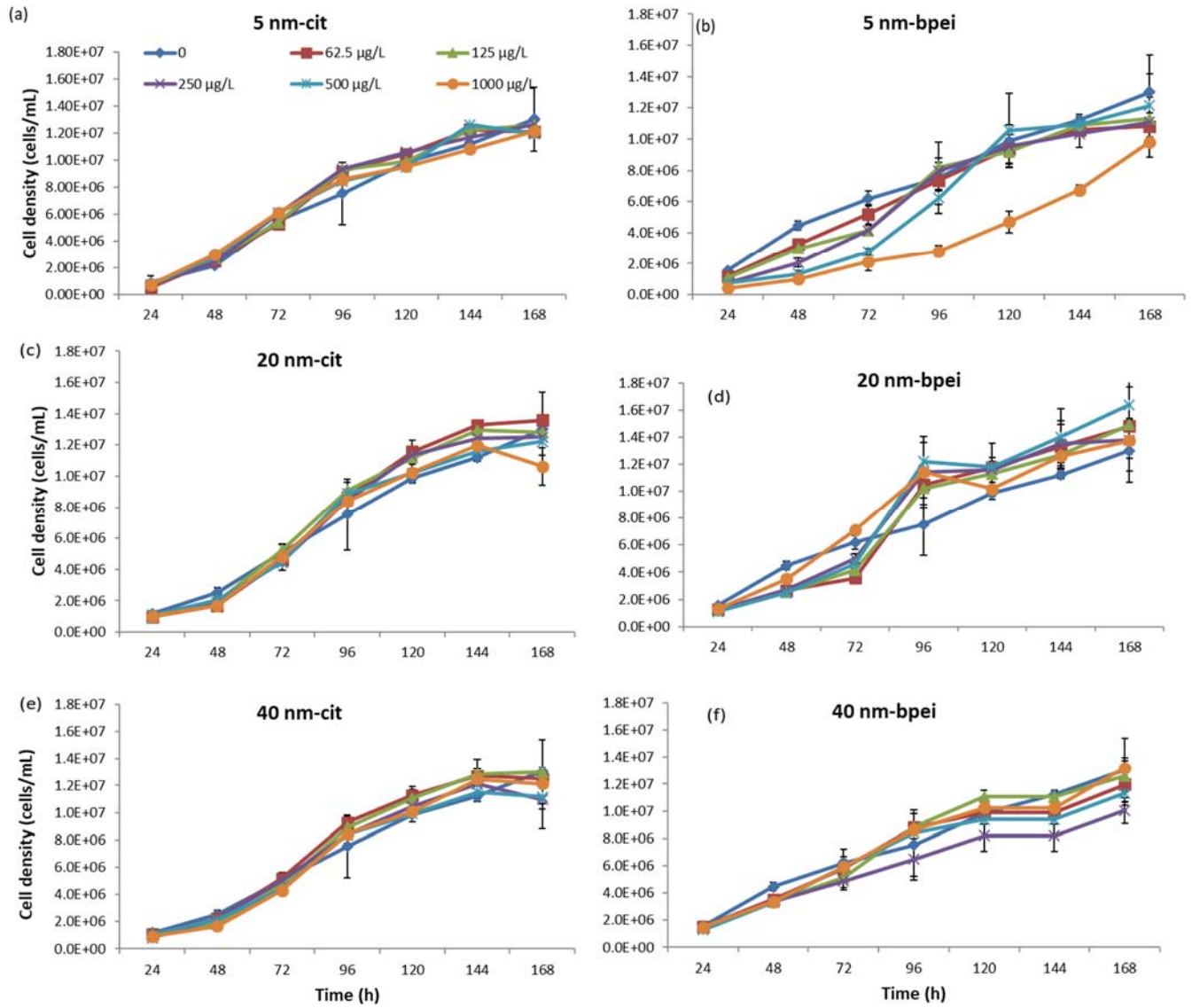


Figure 2: Growth of *P. subcapitata* at different exposure concentrations (0, 62.5, 125, 250, 500, and 1000 µg/L) of nAu. Bars denote standard deviation where $n = 3$. nAu-treated samples were considered significant from the controls when $p < 0.05$.

3.3 Effect of nAu on *P. subcapitata* chl *a* content

For 5 nm cit-, 20 nm cit- and 20 nm BPEI-nAu, photosynthetic pigments (expressed as Chl *a* content) were not significantly different from the controls irrespective of the exposure concentration (Figures 3a, b, e). For both 40 nm-nAu, a significant time-and concentration dependent reduction in Chl *a* content was observed. There was a significant decrease in Chl *a* content at 168 h compared to 72 h at 62.5-1000 $\mu\text{g/L}$ for 40 nm cit-Au (Figure 3 c) and at 500-1000 $\mu\text{g/L}$ for 40 nm-BPEI-Au (Figures 3f). In contrast to growth inhibition observed at 72 h (Figure 2e), significant Chl *a* content promotion was observed compared to the controls for 40 nm cit-Au (Figure 3c). Chl *a* content promotion was likely due to the conversion of other forms of pigments (e.g., Chl *b* content) to Chl *a* content as a response to reactive oxygen species (ROS) following exposure to ENPs (Chen et al., 2012). The decrease in Chl *a* content following exposure to 5 nm BPEI-nAu at 1 000 $\mu\text{g/L}$ (Figure 3d) corresponds with significant algal growth reduction (Figure 2b). Notably, high agglomeration observed for 5 nm BPEI-nAu (HDD = 760 ± 293 nm at 0 h) may have not resulted in a reduction on both surface reactivity and toxicity effects of smaller-sized ENPs. Previously, aggregation did not impede the deleterious effects of ENPs to target organisms (Zakharova et al. 2019). For example, agglomerated nZnO were observed to induce antibacterial effects as their surface activity remained effective (Zakharova et al. 2019). Further, nAu agglomerates were observed to have a shielding effect on algal cells linked to the physical restraint of photons, and thus, inhibiting photosynthesis (Van Hoecke et al. 2009).

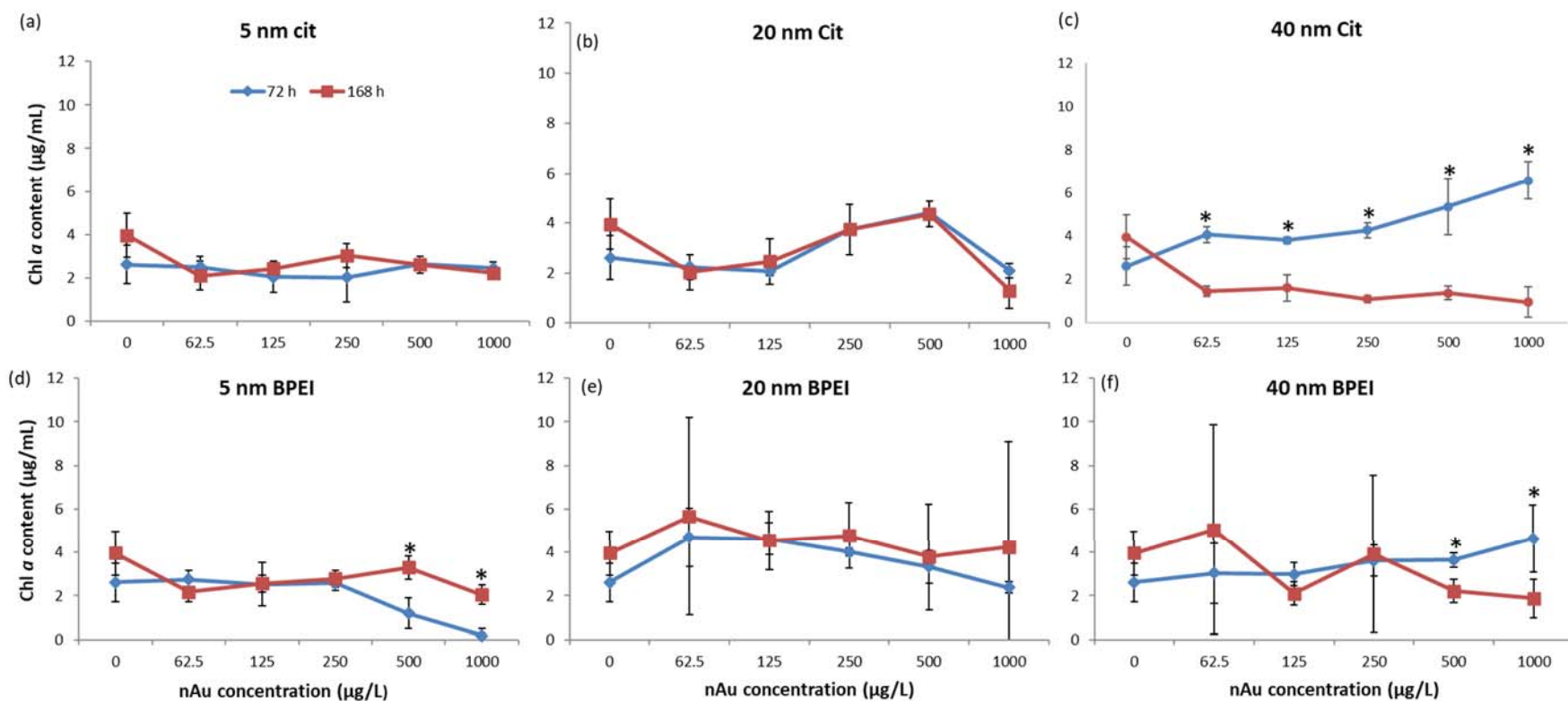


Figure 3: Effect of nAu (0, 62.5, 125, 250, 500, and 1000 µg/L) on Chl *a* content of *P. subcapitata*. Results are reported as mean \pm standard deviation where $n=3$, and * denotes significant differences ($p < 0.05$) between the control and nAu-treated samples at 72 and 168 h.

3.4 Genotoxicity studies

Cytotoxicity studies results did not reveal marked differences between the controls and exposed samples as a function of ENPs exposure concentration (Figures 2 and 3). Herein, the RAPD PCR and AP sites content were used to assess nAu-induced DNA damage on *P. subcapitata*. The genotoxicity studies were done using three concentrations of nAu, viz.: the lowest, median, and highest (62.5, 250, and 1000 µg/L).

3.4.1. RAPD PCR and estimation of genomic template stability

Results in Figure 4 depict the RAPD profiles of isolated genomic DNA from nAu-treated and untreated samples. The profiles were also used to analyse the GTS% (Equation 1). A negative control (no DNA) was included to ascertain whether any band observed was attributable to DNA amplification, or lack thereof. No bands were observed in the negative controls. Loss of normal bands and appearance of new ones relative to the control were observed for nAu exposures conducted using OPB 1 primer (Figure 4 a, b, e, f). For example, in the control five bands were observed, but none were recorded following exposure to 5 nm (62.5 µg/L) and 40 nm (250 µg/L) cit-nAu at 72 h (Figure 4a), and marked reduction in GTS% up to zero value. Using the OPB1 primer, DNA bands with various size ranges were recorded compared to the controls. Irrespective of the nAu coating type and exposure duration, the OPB14 primer produced very similar RAPD profiles (Figures 4c, d, g, and h). Notably, the size range of the genomic bands from cit-nAu exposed samples was different from the controls (Figure 4d and g), thus, evidence of DNA alterations

In previous studies, loss of normal bands was linked to DNA damage including single- and double-strand breaks, modified bases, abasic sites, and/or chromosomal rearrangements (Atienzar et al. 2002; Wolf et al. 2004) following exposure of algae cells to nAu. Conversely, the appearance of new bands was likely due to DNA mutations (Atienzar and Jha 2006). Using OPB1 primer, cit-nAu were observed to induce a reduction in GTS of between 0 and 20% at 72 h. These results are indicative of possible early molecular responses to ENPs directly related to DNA damage (Rocco et al., 2015a). However, likely cell recovery after 168 h was observed as GTS increased to 40-60% for all nAu sizes. Therefore, these findings closely correlate with algal growth promotion observed after 96 h discussed in section 3.2.

Previously, a similar phenomenon was observed in algae (Schiavo et al., 2016) and fish (Rocco et al., 2015a). Schiavo et al., (2016) observed 40 and 55% nuclei damage on algae *Dunaliella tertiolecta* following exposure to 5 and 25 mg Zn/L, respectively, after 24 h using Comet assay. However, after 72 h, no effects were apparent but rather a decrease in the percentage of damaged nuclei relative to 24 h results. Using RAPD-PCR, Rocco et al. (2015a) observed a 37% reduction in GTS following exposure of zebrafish (*Danio rerio*) to nTiO₂ (1 and 10 µg/L) after 14 d, but an increase close to the control after 21-28 d. Both findings were attributed to the activation of defense mechanisms. These findings including our present study highlight the need to consider long-term exposure conditions using molecular approaches. Under short-term exposure, nAu irrespective of type, showed no likelihood of algae recovery as observed under the long-term scenario. This implies that response recovery mechanisms in the short-term were inadequate to protect the algae, and these findings require further investigation. Further, current findings indicate non-recovery of algal cells exposed to 5 nm BPEI-nAu at 1000 µg/L, thus, it is not possible to generalize the ecological implications of ENPs even of the same parent ENPs.

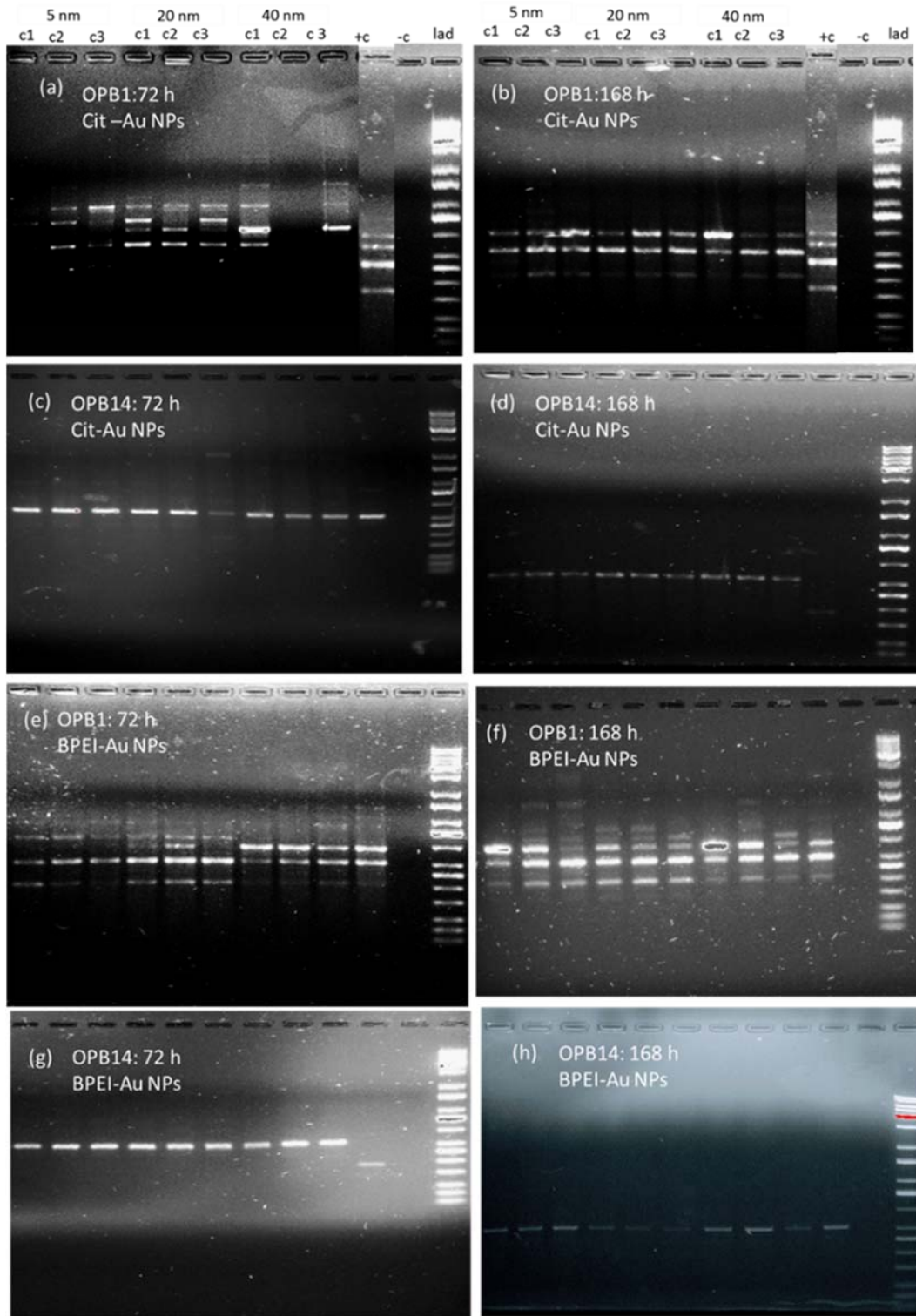


Figure 4: RAPD profiles generated using primers OPB1 and OPB14. Abbreviations: c1- 62.5 $\mu\text{g/L}$, c2- 250 $\mu\text{g/L}$, c3- 1000 $\mu\text{g/L}$, +c- untreated control, -c- negative control (no DNA) and lad- DNA ladder.

3.4.2 Detection of AP sites content

The extent of genotoxicity was determined by comparing the number of AP sites in treated samples to the controls. Results indicated that the AP sites content increased from 15 ± 0.4 per 10^5 bp after 72 h to 18 ± 0.9 AP sites per 10^5 bp at 168 h (Figure 5) in the controls following the method described in Section 2.3.

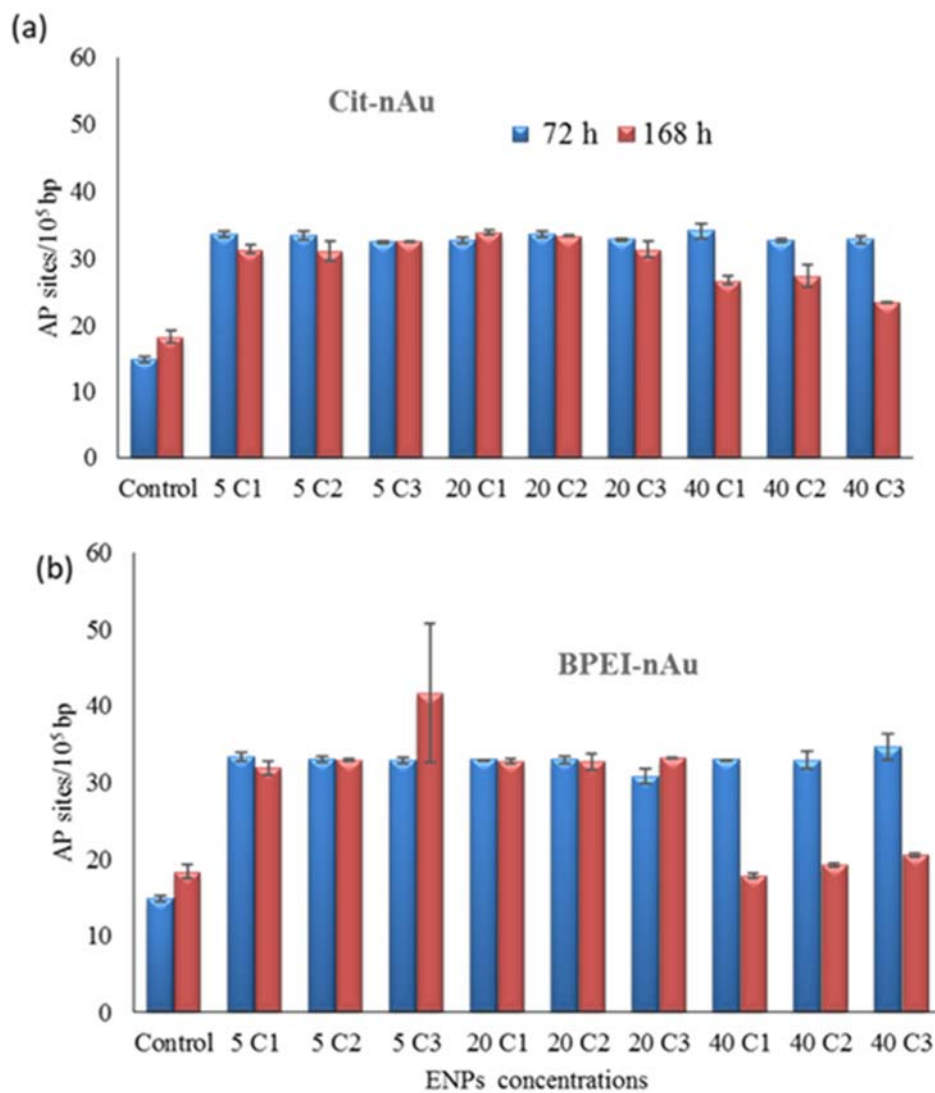


Figure 5: Estimates of AP sites in algal DNA following exposure to nAu at 72 and 168 h using a DNA Damage–AP sites assay. Values are reported as mean \pm standard deviation. C1, C2, and C3 represent nAu concentrations of 62.5, 250, and 1 000 $\mu\text{g/L}$, respectively. The number before the concentration represents nAu size (nm).

A significant increase in AP sites content was observed for cit- and BPEI-nAu treated samples relative to the control after 72 and 168 h (Figure 5) except for 40 nm-sized BPEI nAu after 168 h (Figure 5b). AP sites content over time exhibited significant differences primarily as influenced by ENPs size (no differences at lower sizes (5 and 20 nm) but apparent at higher sizes (40 nm) of nAu). No differences were observed linked to ENPs coating type, or exposure concentration (Figure 5). For example, 40 nm-sized nAu irrespective of coating type and exposure concentration induced a significant reduction of AP sites content after 168 h compared to 72 h (Figure 5a, b). This was attributed to DNA damage recovery under longer chronic exposure of 168 h. These findings correlate with the observed increase in GTS% after 168 h. Moreover, an increase in AP sites content (33 ± 0.4 to 42 ± 9 AP sites per 10^5 bp) was observed after 168 h (Figure 5b) at the highest exposure concentration (1 000 $\mu\text{g/L}$) for 5 nm BPEI-nAu; and were consistent with significant growth inhibition (Figure 2b) and Chl *a* content reduction (Figure 3d) results. Therefore, only 5 nm BPEI-coated-nAu genotoxicity results showed a close correlation with cytotoxicity endpoints (growth inhibition and reduction in Chl *a* content). In turn, this implies it is not plausible to draw generalized implications of ENPs to aquatic organisms even for the same parent material. This is because differences e.g. in size and coating among other influencing factors can underpin the induction of distinctive toxicological outcomes both at physiological and molecular levels.

Similar to cytotoxicity endpoints, results for 40 nm-sized-nAu suggest exposure duration plays a significant role to genetic response of algae to ENPs. Overall, in this study genotoxicity results revealed potential toxicity of nAu to algae at the molecular level even in cases where no effects were apparent at the morphological level. Previously, Geffroy and colleagues (2012) demonstrated that the alteration of genome composition following exposure of *Danio rerio* to nAu (12 and 50 nm) at 36–106 ng Au/fish/d for 60 d. However, Au accumulation in fish tissues was only observed at the highest exposure concentration. Their results showed nAu induced genotoxic effects in fish even where none were observable at the physiological level. Thus, findings herein indicate the significant role of genotoxicity data as a valuable tool for early detection and assessment of potential environmental risks of ENPs to the aquatic biota.

4. Environmental implications

Among aquatic organisms, algae are at the lowest trophic level as producers, providing food and oxygen to other forms of aquatic biota. They also have a high ability for bioaccumulation of pollutants (Bhuvaneshwari et al., 2015). For ENPs exposure, accumulation and transfer to other organisms in the food chain are likely as previously observed for nAg (Lekamge et al., 2019), with a concomitant compromise to the ecological integrity. Herein, results demonstrated that nAu may not cause deleterious effects on algae based on morphological end-points investigations e.g., growth inhibition or chlorophyll content. However, effects may be apparent at the genetic level in the form of DNA damage and/or mutation as our results show. Thus, careful analysis of potential genotoxicity from nano-pollutants for algae should be considered in future studies. Our findings show that DNA damage induced by 40 nm-nAu at 72 h was reversed after 168 h. However, for 5, and 20 nm nAu, DNA damage observed at 72 h persisted after 168 h indicative of complex interplay of ENPs physicochemical properties to the resultant effects.

Findings indicate that smaller-sized nAu may induce higher toxicological outcomes compared to larger-sized ones. DNA damaging pollutants e.g. nAu may interfere with cellular processes resulting in the causation of deleterious effects on the development, growth, and reproduction (Ginebreda et al., 2014). These effects may be carried over to the next generations (Deavaux et al., 2011) where they can compromise both ecological and human health. Understanding the effects of ENPs at lower trophic levels could help predict their potential risks to human health. For example, the potential risk of ENPs to aquatic biota can be transferred to humans via the food chain e.g. through plants and protein diet such as fish. Therefore, there is a strong necessity for genotoxicity studies carried out at environmentally relevant ENPs concentrations (in ng/L to a lower scale of $\mu\text{g/L}$), and secondly, using actual environmental matrixes e.g. freshwater from rivers, wetlands, lakes, etc. Such studies are essential to aid understand ENPs mechanisms of toxicity, especially under chronic conditions to aquatic biota as well as human health.

5. Conclusions

Significant inhibitive cytotoxic effects to algae were only observable following exposure to 5 nm BPEI-nAu at 1 000 $\mu\text{g/L}$, thus indicative of complex interplay between size, coating type, and exposure concentration as influencing factors. All permutations of nAu used in this study induced

inhibitive genotoxic effects irrespective of time, size, coating type, and exposure concentration. Thus, the findings indicate the significant role of genotoxicity studies in assessing the potential environmental risks of ENPs to aquatic biota because assays used are more sensitive compared to those for cytotoxicity investigations.

RAPD-PCR results revealed changes in the DNA of nAu-exposed algae in the form of appearance and/or disappearance of normal bands compared to the controls. Genomic template stability signifying a decrease in DNA stability was observed at a short time of 72 h, but increased after 168 h. Similarly, a significant increase in AP sites content was observed for nAu -treated samples relative to the control after 72 h, but a decrease was observed for 40 nm-sized nAu after 168 h. Overall, in this study, the genotoxicity of nAu to *P. subcapitata* was influenced by nAu size, surface coating type, exposure concentration, and duration. This study provides evidence for the influence of nAu physicochemical properties, and exposure duration on genotoxicity to *P. subcapitata*. This plays a vital role in understanding the behavior and toxicological outcomes of nAu in the aquatic environment.

CRedit author contribution statement

Ntombikayise Mahaye: Investigation; Methodology; Validation; Writing - Original Draft; Data Curation; Formal analysis, Writing – Review & Editing

Samuel K Leareng: Methodology; Validation; Data Curation; Formal Analysis; Writing - Review & Editing

Ndeke Musee: Conceptualization; Funding Acquisition; Project Administration; Resources; Supervision; Writing - Review & Editing

Acknowledgements

The authors acknowledge the financial support from the South African National Research Foundation, Department of Science and Technology Professional Development Programme Doctoral grant (N Mahaye; N Musee), the Council for Scientific and Industrial Research (CSIR) (N Mahaye) where experiments were undertaken, and the University of Pretoria (N Mahaye, SK Leareng, N Musee). We acknowledge Miss Liesl Hill from the CSIR for assisting

with algal growth experiments. The valuable comments and suggestions of three anonymous reviewers which greatly improved the quality of this manuscript are highly acknowledged. We thank Dr Melusi Thwala (CSIR, South Africa) for reviewing the manuscript for grammar.

References

Amaeze NH, Schnell S, Sozeri O, Otitolaju AA, Egonmwan RI, Arlt VM, Bury NR. 2015. Cytotoxic and genotoxic responses of the RTgill-W1 fish cells in combination with the yeast oestrogen screen to determine the sediment quality of Lagos lagoon *Niger*. *Mutagen*, 30(1):117–127.

Amjady F, Golestani EB, Karimi F, Sevda T. 2016. An investigation of the effect of copper oxide and silver nanoparticles on *E. coli* genome by RAPD molecular markers. *Advances in Biotechnology and Microbiology*, 1(2): 555-559.

Anantha AN, Daniel SCGK, Sironmani TA, Umapathia S. 2011. PVA and BSA stabilized silver nanoparticles based surface-enhanced plasmon resonance probes for protein detection. *Colloids and Surfaces B: Biointerfaces*, 85: 138–144.

Angel BM, Vallotton P, Apte SC. 2015. On the mechanism of nanoparticulate CeO₂ toxicity to freshwater algae. *Aquatic Toxicology*, 168: 90–97.

ANSES, 2014. Enjeux et mise à jour des connaissances.

Aruoja V, Pokhrel S, Sihtmäe M, Mortimer M, Mädler L, Kahru A. 2015. Toxicity of 12 metal-based nanoparticles to algae, bacteria and protozoa. *Environmental Science Nano*, 2: 630–644.

Atienzar FA and Jha AN. 2006. The random amplified polymorphic DNA (RAPD) assay and related techniques applied to genotoxicity and carcinogenesis studies: a critical review. *Mutation Research*, 613: 76–102.

Atienzar FA, Venier P, Jha AN, Depledge MH. 2002. Evaluation of the random amplified polymorphic DNA (RAPD) assay for the detection of DNA damage and mutations. *Mutation Research*, 521: 151–163.

- Barbas CF, Burton DR, Scott JK, Silverman GJ. 2007. Quantitation of DNA and RNA. *Cold Spring Harbor Protocols*, 2007(11):pdb-ip47.
- Bayat N, Lopes VR, Scholermann J, Jensen LD, Cristobal S. 2015. Vascular toxicity of ultra-small TiO₂ nanoparticles and single walled carbon nanotubes *in vitro* and *in vivo*. *Biomaterials*, 63: 1-13.
- Bodelón G, Costas C, Pérez-Juste J, Pastoriza-Santos I, Luis M. Liz-Marzán LM. 2017. Gold nanoparticles for regulation of cell function and behaviour. *Nano Today*, 13: 40–60.
- Bolognesi C, Hayashi M. 2011. Micronucleus assay in aquatic animals. *Mutagenesis*, 26 (1): 205–213.
- Bolognesi C, Cirillo S. 2014. Genotoxicity biomarkers in aquatic bioindicators. *Current Zoology*, 60 (2): 273-284.
- Boturyn D, Constant J-F, Defrancq E, Lhomme J, Barbin A, Wild CP. 1999. A simple and sensitive method for *in vitro* quantitation of abasic sites in DNA. *Chemical Research in Toxicology*, 12: 476-482.
- Bhuvaneshwari M, Iswarya V, Archana S, Madhu GM, Kumar GS, Nagarajan R, Chandrasekaran N, Mukherjee A. 2015. Cytotoxicity of ZnO NPs towards fresh water algae *Scenedesmus obliquus* at low exposure concentrations in UV-C, visible and dark conditions. *Aquatic Toxicology*, 162:29-38.
- Caballero-Guzman A, Nowack B. 2018. Prospective nanomaterial mass flows to the environment by life cycle stage from five applications containing CuO, DPP, FeOx, CNT and SiO₂. *Journal of Cleaner Production*, 203: 990-1002.
- Cao PF, Rong LH, de Leon A, Su Z, Advincula RC. 2015. A supramolecular polyethylenimine-cored carbazole dendritic polymer with dual applications. *Macromolecules*, 48: 6801–6809.
- Châtel A, Mouneyrac C. 2017. Signaling pathways involved in metal-based nanomaterial toxicity towards aquatic organisms. *Comparative Biochemistry and Physiology, Part C: Toxicology and Pharmacology*, 196: 61–70.

Chen L, Zhou L, Liu Y, Deng S, Wu H, Wang G. 2012. Toxicological effects of nanometer titanium dioxide (nano-TiO₂) on *Chlamydomonas reinhardtii*. *Ecotoxicology and Environmental Safety*, 84: 155–162.

Chen G, Vijver MG, Peijnenburg WJ. 2015. Summary and analysis of the currently existing literature data on metal-based nanoparticles published for selected aquatic organisms: Applicability for toxicity prediction by (Q) SARs. *Alternatives to Laboratory Animals*, 43(4):221-40.

Chen X, Zhang C, Tan L, Wang J. 2018. Toxicity of Co nanoparticles on three species of marine microalgae. *Environmental Pollution*, 236: 454-461.

Chen Y, Chen L, Wu Y, Di J. 2019. Highly sensitive determination of dopamine based on the aggregation of small-sized gold nanoparticles. *Microchemical Journal*, 147:955-961.

Cho TJ, Gorham JM, Pettibone JM, Liu J, Tan J, Hackley VA. 2019. Parallel multi-parameter study of PEI-functionalized gold nanoparticle synthesis for bio-medical applications: part 1—a critical assessment of methodology, properties, and stability. *Journal of Nanoparticle Research*, 21(8):188.

Clemente Z, Castro VL, Feitosa LO, Lima R, Jonsson CM, Maia AHN, Fraceto LF. 2013. Fish exposure to nano-TiO₂ under different experimental conditions: Methodological aspects for nanoecotoxicology investigations. *Science of the Total Environment*, 463–464: 647–656.

Copland JA, Eghtedari M, Popov VL, Kotov N, Mamedova N, Motamedi M, Oraevsky AA. 2004. Bioconjugated gold nanoparticles as a molecular based contrast agent: implications for imaging of deep tumors using optoacoustic tomography. *Molecular Imaging and Biology*, 6(5):341-349.

Danabas D, Ates M, Tastan BE, Cimen IC, Unal I, Aksu O, Kutlu B. 2020. Effects of Zn and ZnO nanoparticles on *Artemia salina* and *Daphnia magna* organisms: toxicity, accumulation and elimination. *Science of the Total Environment*, 711:134869.

de Alteriis E, Falanga A, Galdiero S, Guida M, Maselli V, Galdiero E. 2018. Genotoxicity of gold nanoparticles functionalized with indolicidin towards *Saccharomyces cerevisiae*. *Journal of Environmental Sciences*, 66:138 – 145.

Dědková K, Bures Z, Palarcík J, Vlcek M, Kukutschova J. 2014. Acute toxicity of gold nanoparticles to freshwater green algae. In: Conference NanoCon, Nov 5th -7th, Brno, Czech Republic.

Demir E, Kaya N, Kaya B. 2014. Genotoxic effects of zinc oxide and titanium dioxide nanoparticles on root meristem cells of *Allium cepa* by comet assay. *Turkish Journal of Biology*, 38: 31-39.

Demple B, Harrison L. 1994. Repair of oxidative damage to DNA: enzymology and biology. *Annual Review of Biochemistry*, 63:915–948.

El-Sayed IH, Huang X, El-Sayed MA. 2005. Surface plasmon resonance scattering and absorption of anti-EGFR antibody conjugated gold nanoparticles in cancer diagnostics: applications in oral cancer. *Nano letters*, 5(5):829-834.

Feng B, Wang K, Yang Y, Wang G, Zhang H, Liu Y, Jiang K. 2019. Ultrasensitive recognition of AP sites in DNA at the single-cell level: one molecular rotor sequentially self-regulated to form multiple different stable conformations. *Chemical science*, 10(44), pp.10373-10380.

Gao C, De Schampheleere KAC, Smolders E. 2016. Zinc toxicity to the alga *Pseudokirchneriella subcapitata* decreases under phosphate limiting growth conditions. *Aquatic Toxicology*, 173: 74–82.

Ginebreda A, Kuzmanovic M, Guasch H, de Alda ML, López-Doval JC, Muñoz I, Ricart M, Romaní AM, Sabater S, Barceló D. 2014. Assessment of multi-chemical pollution in aquatic ecosystems using toxic units: compound prioritization, mixture characterization and relationships with biological descriptors. *Science of the total environment*, 468:715-723.

Ghazaei F, Shariati M. 2020. Effects of titanium nanoparticles on the photosynthesis, respiration, and physiological parameters in *Dunaliella salina* and *Dunaliella tertiolecta*. *Protoplasma*, 257(1):75-88.

Geffroy B, Ladhar C, Cambier S, Treguer-Delapierre M, Brèthes D, Bourdineaud J-P. 2012. Impact of dietary gold nanoparticles in zebrafish at very low contamination pressure: The role of size, concentration and exposure time. *Nanotoxicology*, 6:2: 144-160.

Golbamaki N, Rasulev B, Cassano A, Robinson RLM, Benfenati E, Leszczynski J, Cronin MTD. 2015. Genotoxicity of metal oxide nanomaterials: review of recent data and discussion of possible mechanisms. *Nanoscale*, 7: 2154-2198.

Hansen SF, Heggelund LR, Besora PR, Mackevica A, Boldrin A, Baun A. 2016. Nanoproducts: what is actually available to European consumers? *Environmental Science Nano*, 3: 169–180.

Hitchman A, Smith GH, Ju-Nam Y, Sterling M, Lead JR. 2013. The effect of environmentally relevant conditions on PVP stabilised gold nanoparticles. *Chemosphere*, 90(2):410-416.

Iswarya V, Manivannan J, De A, Paul S, Roy R, Johnson JB, Kundu R, Chandrasekaran N, Mukherjee A, Mukherjee A. 2016. Surface capping and size-dependent toxicity of gold nanoparticles on different trophic levels. *Environmental Science and Pollution Research*, 23:4844–4858.

Jang J, Huh YJ, Cho HJ, Lee B, Park J, Hwang DY, Kim DW. 2017. SIRT1 enhances the survival of human embryonic stem cells by promoting DNA repair. *Stem cell reports*, 9(2):629-41.

Ji J, Long Z and Lin D. 2011. Toxicity of oxide nanoparticles to the green algae *Chlorella sp.* *Chemical Engineering Journal*, 170: 525–530.

Jiang Z, Sun S, Liang A, Huang W, Qin A. 2006. Gold-labeled nanoparticle-based immunoresonance scattering spectral assay for trace apolipoprotein AI and apolipoprotein B. *Clinical Chemistry*, 52(7):1389-1394.

Kahru A, Dubourguier HC. 2010. From ecotoxicology to nanoecotoxicology. *Toxicology*, 269(2-3):105-119.

Kalman J, Paul KB, Khan FR, Stone V, Fernandes TF. 2015. Characterisation of bioaccumulation dynamics of three differently coated silver nanoparticles and aqueous silver in a simple freshwater food chain. *Environmental Chemistry*, 12: 662-672.

Kim I, Lee B, Kim H, Kim K, Kim SD, Hwang Y. 2016. Citrate coated silver nanoparticles change heavy metal toxicities and bioaccumulation of *Daphnia magna*. *Chemosphere*, 143: 99–105.

Klaine SJ, Alvarez PJJ, Batley GE, Fernandes TF, Handy RD, Lyon DY, Mahendra S, McLaughlin MJ, Lead JR. 2008. Nanomaterials in the environment: behavior, fate, bioavailability, and effects. *Environmental Toxicology and Chemistry*, 27(9): 1825-1851.

Kleiven M, Macken A, Oughton DH. 2019. Growth inhibition in *Raphidocelis subcapitata*—Evidence of nanospecific toxicity of silver nanoparticles. *Chemosphere*, 221:785-792.

Koehlé-Divo V, Cossu-Leguille C, Pain-Devin S, Simonin C, Bertrand C, Sohm B, Mouneyrac C, Devin S, Giambérini L. 2018. Genotoxicity and physiological effects of CeO₂ NPs on a freshwater bivalve (*Corbicula fluminea*). *Aquatic Toxicology*, 198: 141-148.

Kuczyńska-Wiśnik D, Stojowska K, Matuszewska E, Leszczyńska D, Algara MM, Augustynowicz M, Laskowska E. 2015. Lack of intracellular trehalose affects formation of *Escherichia coli* persister cells. *Microbiology*, 161(4):786-96.

Lekamge S, Miranda AF, Ball AS, Shukla R, Nugegoda D. 2019. The toxicity of coated silver nanoparticles to *Daphnia carinata* and trophic transfer from alga *Raphidocelis subcapitata*. *PLoS one*, 14(4).

Liu Y, Dai J, Xu L, Liu X, Liu J, Li G. 2016. Red to brown to green colorimetric detection of Ag⁺ based on the formation of Au-Ag core-shell NPs stabilized by a multi-sulfhydryl functionalized hyperbranched polymer. *Sensors and Actuators B*, 237: 216–223.

Loeb LA, Preston BD. 1986. Mutagenesis by apurinic/ apyrimidinic sites. *Annual Review of Genetics*, 20: 201-230.

Lowry GV, Hill RJ, Harper S, Rawle AF, Hendren CO, Klaessig F, Nobbmann U, Sayre P, Rumble J. 2016. Guidance to improve the scientific value of zeta-potential measurements in nanoEHS. *Environmental Science: Nano*, 3(5):953-965.

Magdolenova Z, Collins A, Kumar A, Dhawan A, Stone V, Dusinska M. 2014. Mechanisms of genotoxicity. A review of in vitro and in vivo studies with engineered nanoparticles. *Nanotoxicology*, 8(3): 233-278.

Mahaye N, Thwala M, Cowan DA, Musee N. 2017. Genotoxicity of metal based engineered nanoparticles in aquatic organisms: A review. *Mutation Research Reviews, Mutation Research*, 773: 134–160.

Mahaye N. 2019. Stability of gold and cerium oxide nanoparticles in aqueous environments, and their effects on *Pseudokirchneriella subcapitata* and *Salvinia minima* (Doctoral dissertation, University of Pretoria). <https://repository.up.ac.za/handle/2263/72778>

Manna I and Bandyopadhyay M. 2017. Engineered nickel oxide nanoparticles affect genome stability in *Allium cepa* (L.). *Plant physiology and biochemistry*, 121, pp.206-215.

Musee N. 2011. Simulated environmental risk estimation of engineered nanomaterials: A case of cosmetics in Johannesburg City. *Human and Experimental Toxicology*, 30(9): 1181-1195.

Musee N, Leareng S, Kebaabetswe L, Tubatsi G, Mahaye N, Thwala M. 2020. Implications of surface coatings on engineered nanomaterials for environmental systems: status quo, challenges, and perspectives. In *Handbook of Functionalized Nanomaterials for Industrial Applications*, Elsevier: 399-416.

Nanogenotox, 2013. Facilitating the safety evaluation of manufactured nanomaterials by characterizing their potential genotoxic hazard. Online: www.nanogenotox.eu.

Nyati S, Werth S, Honegger R. 2013. Genetic diversity of sterile cultured *Trebouxia* photobionts associated with the lichen-forming fungus *Xanthoria parietina* visualized with RAPD-PCR fingerprinting techniques. *The Lichenologist*, 45(6):825-840.

Oberholster PJ, Hill L, Jappie S, Truter JC, Botha AM. 2016. Applying genotoxicology tools to identify environmental stressors in support of river management. *Chemosphere*, 144:319-329.

O'Brien RW, White LR. 1978. Electrophoretic mobility of a spherical colloidal particle. *Journal of the Chemical Society, Faraday Transactions 2: Molecular and Chemical Physics*, 74:1607-1626.

Organisation for Economic Cooperation and Development. Algal growth inhibition test. OECD guidelines for testing of chemicals 201. Paris, France; 1984.

- Peters RJB, van Bommel G, Milani NBL, den Hertog GCT, Undas AK, van der Lee M, Bouwmeester H. 2018. Detection of nanoparticles in Dutch surface waters. *Science of the Total Environment*, 621: 210–218.
- Perreault F, Oukarroum A, Melegari SP, Matias WG, Popovic R. 2012. Polymer coating of copper oxide nanoparticles increases nanoparticles uptake and toxicity in the green alga *Chlamydomonas reinhardtii*. *Chemosphere*, 87(11):1388-1394.
- Piccinno F, Gottschalk F, Seeger S, Nowack B. 2012. Industrial production quantities and uses of ten engineered nanomaterials for Europe and the world. *Journal of Nanoparticle Research*, 14: 1109–1120.
- Qiang L, Arabeyyat ZH, Xin Q, Paunov VN, Dale IJ, Lloyd Mills RI, Rotchell JM, Cheng J. 2020. Silver nanoparticles in Zebrafish (*Danio rerio*) embryos: uptake, growth and molecular responses. *International Journal of Molecular Sciences*, 21(5):1876.
- Qiu TA, Bozich JS, Lohse SE, Vartanian AM, Jacob LM, Meyer BM, Gunsolus IL, Niemuth NJ, Murphy CJ, Haynes CL, Klaper RD. 2015. Gene expression as an indicator of the molecular response and toxicity in the bacterium *Shewanella oneidensis* and the water flea *Daphnia magna* exposed to functionalized gold nanoparticles. *Environmental Science: Nano*, 2(6):615-629.
- Rocco L, Santonastaso M, Mottola F, Costagliola D, Suero T, Pacifico S, Stingo V. 2015a. Genotoxicity assessment of TiO₂ nanoparticles in the teleost *Danio rerio*. *Ecotoxicology and Environmental Safety*, 113: 223–230.
- Rocco L, Santonastaso M, Nigro M, Mottola F, Costagliola D, Bernardeschi M, Guidi P, Lucchesi P, Scarcelli V, Corsi I, Stingo V. 2015b. Genomic and chromosomal damage in the marine mussel *Mytilus galloprovincialis*: Effects of the combined exposure to titanium dioxide nanoparticles and cadmium chloride. *Marine environmental research*, 111:144-148.
- Rodrigues LHR, Arenzon A, Raya-Rodriguez MT, Fontoura NF. 2011. Algal density assessed by spectrophotometry: A calibration curve for the unicellular algae *Pseudokirchneriella subcapitata*. *Journal of Environmental Chemistry and Ecotoxicology*, 3(8):225-228.

Rogers NJ, Franklin NM, Apte SC, Batley GE, Angel BM, Lead JR, Baalousha M. 2010. Physico-chemical behaviour and algal toxicity of nanoparticulate CeO₂ in freshwater. *Environmental Chemistry*, 7: 50–60.

Sadiq IM, Pakrashi S, Chandrasekaran N, Mukherjee A. 2011. Studies on toxicity of aluminium oxide (Al₂O₃) nanoparticles to microalgae species: *Scenedesmus* sp. and *Chlorella* sp. *Journal of Nanoparticle Research*, 13 (8): 3287-3299.

Samadian H, Salami MS, Jaymand M, Azarnezhad A, Najafi M, Barabadi H, Ahmadi A. 2020. Genotoxicity assessment of carbon-based nanomaterials; Have their unique physicochemical properties made them double-edged swords? *Mutation Research/Reviews in Mutation Research*:108296.

Schiavo S, Oliviero M, Miglietta M, Rametta G, Manzo S. 2016. Genotoxic and cytotoxic effects of ZnO nanoparticles for *Dunaliella tertiolecta* and comparison with SiO₂ and TiO₂ effects at population growth inhibition levels. *Science of the Total Environment*, 550: 619–627.

Scown TM, van Aerle R, Tyler CR. 2010. Review: Do engineered nanoparticles pose a significant threat to the aquatic environment? *Critical Reviews in Toxicology*, 40(7): 653–670.

Seiple LA, Cardellina JH, Akee R, Stivers JT. 2008. Potent inhibition of human apurinic/apyrimidinic endonuclease 1 by arylstibonic acids. *Molecular pharmacology*, 73(3):669-677.

Sen GT, Ozkemahli G, Shahbazi R, Erkekoglu P, Ulubayram K, Kocer-Gumusel B. 2020. The effects of polymer coating of gold nanoparticles on oxidative stress and DNA damage. *International Journal of Toxicology*, 39(4):328-340.

Sendra M, Sánchez-Quiles D, Blasco J, Moreno-Garrido I, Lubiána LM, Pérez-García S, Tovar-Sánchez A. 2017. Effects of TiO₂ nanoparticles and sunscreens on coastal marine microalgae: Ultraviolet radiation is key variable for toxicity assessment. *Environment International*, 98: 62–68.

Slabbert, L. 2004. Methods for Direct Estimation of Ecological Effect Potential (DEEEP). First Edition. Water Research Commission Report No.: 1313/01/04. Water Research Commission, Pretoria, South Africa. 100 pages.

Thompson DT. 2007. Using gold nanoparticles for catalysis. *Nanotoday*, 2(4): 40-43.

US EPA. 1978. The *Selenastrum capricornutum* Printz algal assay bottle test: Experimental design, application and data interpretation. EPA/600/9-78/018. US Environmental Protection Agency, Corvallis.

US EPA. 1989. Short-term methods for estimating the chronic toxicity of effluents and receiving waters to freshwater organisms. Second Edition. EPA/600/4-89/001. Environmental Monitoring Systems Laboratory, Office of Research and Development, US Environmental Protection Agency, Cincinnati.

Vales G, Siivola KM, Suhonen S, Savolainen KM, Norppa H, Catalán J. 2020. Size, surface functionalization, and genotoxicity of gold nanoparticles in vitro. *Nanomaterials*, 10(2):271.

Van Hoecke K, Quik JTK, Mankiewicz-Boczek J, De Schamphelaere KAC, Elsaesser A, Van der Meeren P, Barnes C, McKerr G, Howard CV, Van DeMeent D, Rydzynski K, Dawson KA, Salvati A, Lesniak A, Lynch I, Silversmit G, De Samber B, Vincze L, Janssen CR. 2009. Fate and effects of CeO₂ nanoparticles in aquatic ecotoxicity tests. *Environmental Science and Technology*, 43:4537–4546.

Wang D, Zhao R, Qu YY, Mei XY, Zhang X, Zhou Q, Li Y, Yang SB, Zuo ZG, Chen YM, Lin Y. 2018. Colonic lysine homocysteinylation induced by high-fat diet suppresses DNA damage repair. *Cell reports*, 25(2):398-412.

Wolf HD, Blust R, Backeljau T. 2004. The use of RAPD in ecotoxicology. *Mutation Research*, 566: 249–262.

Zakharova O, Kolesnikov E, Vishnyakova E, Strekalova N, Gusev A. 2019. Antibacterial activity of ZnO nanoparticles: dependence on particle size, dispersion media and storage time. IOP Conference Series: *Earth and Environmental Science*, 226: 012062.

Załęska-Radziwiłł M, Doskocz N. 2016. DNA changes in *Pseudomonas putida* induced by aluminium oxide nanoparticles using RAPD analysis. *Desalination and Water Treatment*, 57(3): 1573-1581.

Zhang J, Xiang Q, Shen L, Ling J, Zhou C, Hu J, Chen L. 2020. Surface charge-dependent bioaccumulation dynamics of silver nanoparticles in freshwater algae. *Chemosphere*, 247:125936.

Zhao J, Lin M, Wang Z, Cao X, Xing B. 2020. Engineered nanomaterials in the environment: Are they safe? *Critical Reviews in Environmental Science and Technology*:1-36.